Surface anisotropy from photo-induced bond breaking at polymer surfaces: A sum-frequency vibrational spectroscopic study of polyimide

ARTICLE *in* THE JOURNAL OF CHEMICAL PHYSICS · SEPTEMBER 2001

Impact Factor: 2.95 · DOI: 10.1063/1.1391480

3 AUTHORS, INCLUDING:

Doseok Kim
Sogang University
122 PUBLICATIONS **2,131** CITATIONS
SEE PROFILE

yi-ren Shen
China Medical University (ROC)
249 PUBLICATIONS **10,467** CITATIONS
SEE PROFILE

Surface anisotropy from photo-induced bond breaking at polymer surfaces: A sum-frequency vibrational spectroscopic study of polyimide

Masahito Oh-e, Doseok Kim,[a] and Y. R. Shen[b]
Department of Physics, University of California at Berkeley, Berkeley, California 94720

(Received 30 April 2001; accepted 19 June 2001)

Sum-frequency vibrational spectroscopy was used to study how linearly polarized UV irradiation could cause bond breaking and alter the surface structure of a polyimide. The spectroscopic results allowed the determination of an approximate orientational distribution of the polymer backbones at a rubbed surface. They also permitted deduction of rates of bond breaking of the backbones at the surface by UV dosage. The surface anisotropy resulting from bond breaking by linearly polarized UV irradiation was found to be relatively small, suggesting a weak azimuthal anchoring energy for liquid crystal films deposited on such a surface. © *2001 American Institute of Physics.* [DOI: 10.1063/1.1391480]

I. INTRODUCTION

Liquid crystal (LC) devices require proper control of LC molecular alignment at the macroscopic level. Presently, such an alignment is most commonly achieved by mechanical rubbing of polymer-coated substrates.[1,2] The rubbed polyimide (PI) surface aligns an LC monolayer adsorbed on it via short-range interaction, which in turn aligns an LC bulk via LC molecular correlation.[3–9] This scheme, however, has some unwanted features in the manufacturing process. Alternative methods capable of aligning LC films have attracted much attention. Among them are the photo-induced alignment techniques. They can be classified into three types based on the photo-induced reactions involved, namely, isomerization,[10,11] dimerization[12–14] and decomposition.[15–18] In the work reported here, we focus our study on the last technique. It has been demonstrated that a PI film irradiated by linearly polarized UV light (LPL) can be used as a surface alignment layer to yield a homogeneous LC bulk alignment in the direction perpendicular to the linear polarization. A plausible explanation for the alignment is that the LPL would preferentially break the PI backbones lying parallel to the UV polarization at the surface.[15,17,18] This picture, however, has not yet been substantiated. In particular, it is not clear which parts of PI at the surface are actually decomposed by UV irradiation.

Infrared (IR) spectroscopy has been used to study photo-induced decomposition and structural anisotropy by LPL in a PI film, and bond breaking by UV irradiation has been observed.[19,20] However, the surface layer probed in this case was not of a monolayer, but of a layer a few nm deep. We used infrared-visible sum-frequency generation (SFG) vibrational spectroscopy in our study since the technique has been proven to be a powerful surface analytical probe.[21,22] It is highly surface-specific and has a submonolayer sensitivity. The surface specificity arises because under the electric-dipole approximation, SFG is forbidden in media with inversion symmetry, but allowed at a surface or interface where such symmetry is broken.[23] If the infrared input is scanned over interfacial vibrational resonances, SFG from the interface is resonantly enhanced. This then yields a vibrational spectrum for the interface. The surface vibrational spectra with different input/output polarizations allow probing of selected atomic groups appearing at the surface. They can provide, for example, information about surface structure and composition of a polymer.

We report in this paper the results of our SFG spectroscopic study to probe rubbed and unrubbed PI surfaces and to detect how they are modified by irradiation of LPL. We found that UV irradiation breaks the C=O and C–C bonds in the PI main chains. Our spectroscopic results provide quantitative information on how the PI main chains were aligned on rubbed and unrubbed surfaces and how rapidly they were broken by UV irradiation. It was found that the resulting surface anisotropy from preferential bond breading by linearly polarized UV light parallel or perpendicular to the PI backbones is small. This suggests that the azimuthal anchoring energy for LC films deposited on such a surface would be small.

II. THEORETICAL BACKGROUND

The basic theory of SFG for surface studies has been described elsewhere.[24,25] Here, we give a brief account for convenience of later discussion. The surface SFG intensity generated in reflection by the input fields of $E_1(\omega_{\mathrm{vis}})$ and $E_2(\omega_{\mathrm{ir}})$is given by

$$I(\omega_{\mathrm{SF}}) = \frac{8\pi^3 \omega_{\mathrm{SF}}^2 \sec^2 \beta_{\mathrm{SF}}}{c^3} |\chi_{\mathrm{eff}}^{(2)}|^2 |E_1(\omega_{\mathrm{vis}}) E_2(\omega_{\mathrm{ir}})|^2, \quad (1)$$

where β_{SF} is the reflection angle of the SF output. The effective surface nonlinearity $\chi_{\mathrm{eff}}^{(2)}$ takes the form of

[a]Current address: Department of Physics, Sogang University, Seoul, 121–742 Korea.
[b]Author to whom correspondence should be addressed. Electronic mail: shenyr@socrates.berkeley.edu

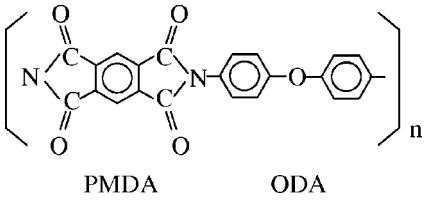

FIG. 1. Chemical structure of polyimide PMDA–ODA used in this study.

$$\chi^{(2)}_{\text{eff}} = [\hat{e}(\omega_{\text{SF}}) \cdot \vec{L}(\omega_{\text{SF}})] \cdot \vec{\chi}^{(2)} : [\hat{e}(\omega_{\text{vis}}) \cdot \vec{L}(\omega_{\text{vis}})] \times [\hat{e}(\omega_{\text{ir}}) \cdot \vec{L}(\omega_{\text{ir}})], \tag{2}$$

with $\hat{e}(\omega)$ being the unit polarization vector and $\vec{L}(\omega)$ the tensorial Fresnel factor at frequency ω. The nonlinear susceptibility $\vec{\chi}^{(2)}$ can be written as

$$\vec{\chi}^{(2)} = \vec{\chi}^{(2)}_{\text{NR}} + \text{N}_s \int \vec{\alpha}^{(2)}(\Omega) f(\Omega) d\Omega, \tag{3}$$

with

$$\vec{\alpha}^{(2)}(\omega_{\text{ir}}, \Omega) = \sum_q \frac{\vec{a}_q(\Omega)}{(\omega_{\text{ir}} - \omega_q) + i\Gamma_q}, \tag{4}$$

such that

$$\vec{\chi}^{(2)}(\omega_{\text{ir}}) = \vec{\chi}^{(2)}_{\text{NR}} + \sum_q \frac{\vec{A}_q}{(\omega_{\text{ir}} - \omega_q) + i\Gamma_q}, \tag{5}$$

with

$$\vec{A}_q = N_s \int \vec{a}_q(\Omega) f(\Omega) d\Omega. \tag{6}$$

Here, N_s is the surface density of contributing atomic groups, $\chi^{(2)}_{\text{NR}}$ denotes the nonresonant contribution, $\alpha^{(2)}_R$ is the resonant hyper-polarizability, $\vec{a}_q$, ω_q, and Γ_q are, respectively, the strength, resonant frequency, and damping constant of the q_{th} resonant mode, Ω represents a set of angles (θ, ϕ, ψ) describing the molecular orientation, and $f(\Omega)$ represents the molecular orientational distribution. In the following, we shall use Eqs. (1)–(6) to fit the observed SFG vibrational spectra and deduce the various characteristic parameters for the surface vibrational modes.

III. EXPERIMENT

In our experiment, the PI (poly[4,4′-oxydiphenylene-pyromellitimide], PMDA–ODA) samples with a layer thickness of ~25 nm were prepared by spin-coating. The chemical structure of PMDA–ODA is shown in Fig. 1. To obtain uniform layers, the PMDA–ODA polyamic acid solution was filtered with membrane filters. It was then dropped on a substrate to be spin-coated at 3500 rpm for 60 seconds. The samples were then baked at 250 °C for 20 minutes for imidization reaction. A 248 nm KrF-excimer laser beam, linearly polarized and homogenized, was used to irradiate the spin-coated PI film. A stack of quartz plates set at the Brewster angle was used as the polarizer. The amount of irradiation was controlled by the beam flux and the number of laser shots. Rubbing of a PI surface was carried out by a rubbing machine with a velvet cloth.

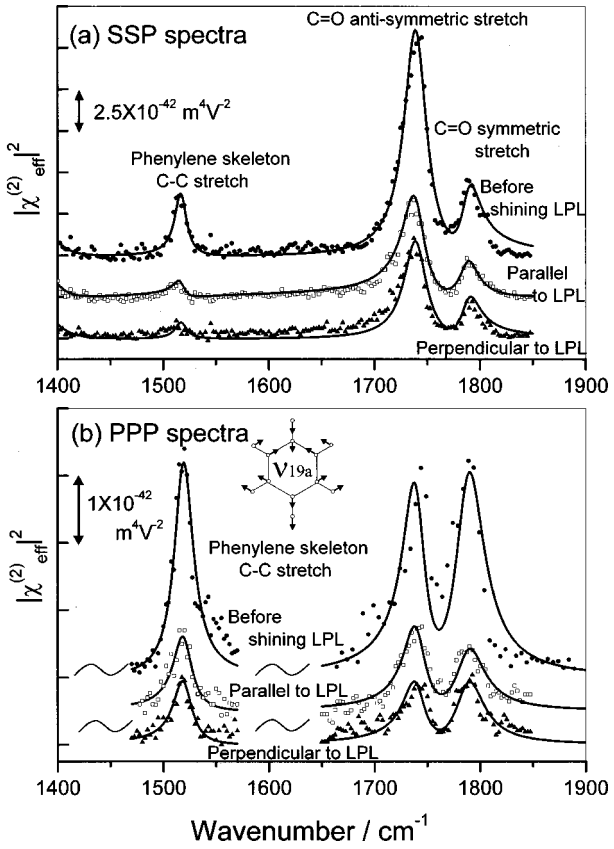

FIG. 2. SFG spectra with (a) SSP and (b) PPP polarization combinations for a PMDA–ODA thin film before and after the linearly polarized UV laser irradiation (30 J/cm^2). The peaks at 1515, 1740, and 1785 cm^{-1} are attributed to the phenylene skeleton C–C stretch, the CO antisymmetric stretch, and CO symmetric stretch modes, respectively. The filled dots describe the spectra before UV irradiation. The empty circles and the triangles describe spectra after UV irradiation with the incidence plane parallel and perpendicular to the UV polarization, respectively. The inset shows the normal mode vibration of the phenylene skeleton stretch mode. The spectra are normalized by the SF signal from a *z*-cut quartz. The parameters for this procedure are listed in Table III.

IV. RESULTS AND DISCUSSION

Shown in Fig. 2(a) are the representative SFG spectra of PMDA–ODA in the range from 1400 to 1850 cm^{-1} before and after LPL irradiation (with the incidence plane parallel and perpendicular to the polarization of UV irradiation in the latter case). The input/output polarization combination was SSP (denoting s-, s-, and p-polarization for SF output, visible input, and IR input, respectively). The sample measured was irradiated by LPL with a total dosage of 30 J/cm^2 obtained from 4000 laser pulses with 7.5 mJ/cm^2 per pulse. Such irradiated PMDA–ODA samples used as substrates for an LC display cell was able to yield a good homogeneous LC bulk alignment perpendicular to the UV polarization. The spectral peaks in Fig. 2(a) can be identified by referring to the IR and Raman spectra of PMDA–ODA: C=O symmetric stretch at ~1785 cm^{-1}, C=O antisymmetric stretch at ~1740 cm^{-1},

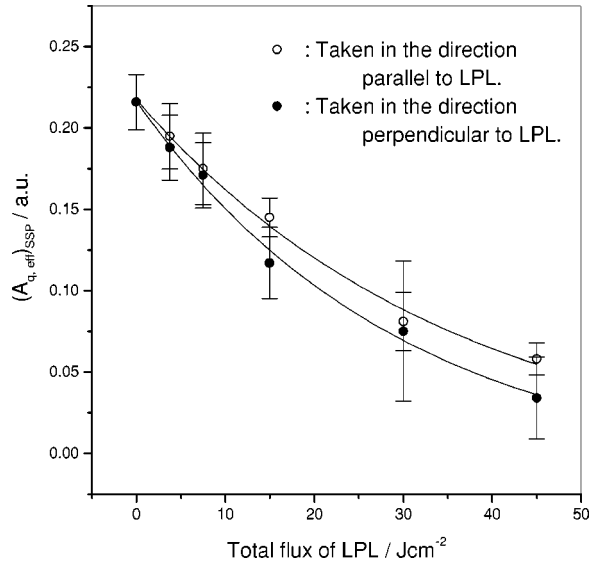

FIG. 3. Decays of the peak amplitude of the phenylene stretch mode as functions the dosage of UV irradiation. The empty and filled circles are data taken with the incidence plane parallel and perpendicular to the UV polarization, respectively.

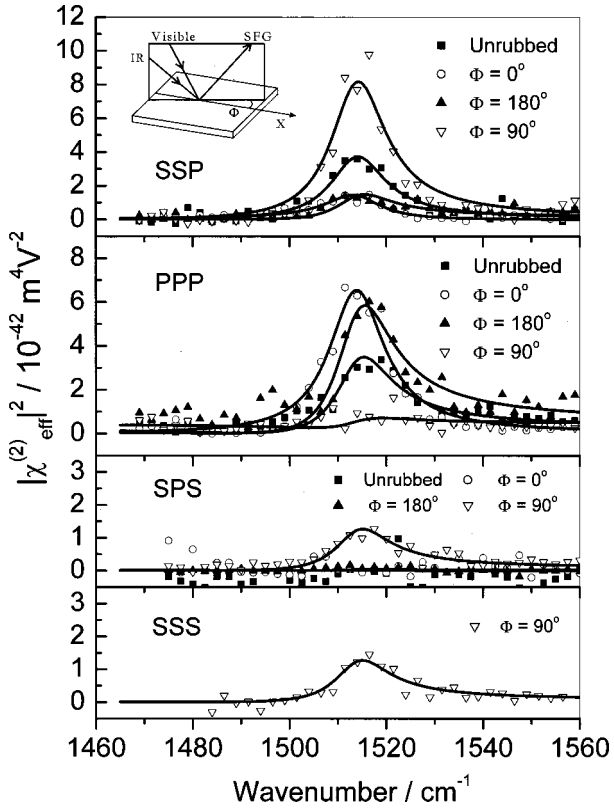

FIG. 4. SFG spectra for a PMDA–ODA thin film before and after rubbing. The angle Φ between the incidence plane and the rubbing direction describes the azimuthal orientation of the sample. The spectra are normalized by the SF signal from a z-cut quartz. The parameters for this procedure are listed in Table III.

and phenylene skeleton C–C stretch at ~1515 cm^{-1}.[26] Figure 2(b) describes the corresponding SFG spectra with the PPP polarization combination. In SPS, the spectral features were too weak to be detected. The spectra in Fig. 2 show that in both SSP and PPP cases, the peak intensities of both phenylene skeleton C–C stretch and C=O stretch modes were significantly reduced by LPL irradiation. The anisotropy seen in the spectra after irradiation is, however, weak.

Similar reduction of spectral peaks by UV irradiation of PI films was observed by IR spectroscopy that lacks surface specificity.[19,20,27] This then indicates that the observed peak reduction in the spectra of Fig. 2 is not due to photo-induced reorientation of the relevant atomic groups, but due to photo-induced bond breaking. Both the C=O bonds in the PMDA part and the C–C bonds in the phenylene skeleton of ODA appear to be broken, suggesting a rather severe fragmentation of the PI backbones by UV irradiation.

If the UV irradiation preferentially breaks the PI backbones lying parallel to the UV polarization, one would expect observation of anisotropy in the SFG spectra. Higher UV dosage should yield a higher degree of anisotropy. Sufficiently large anisotropy in the surface structure would then be able to align an LC bulk film. In our experiment, we vary the UV dosage by varying the number of irradiating UV laser pulses, keeping the flux per pulse constant at 7.5 mJ/cm^2. At 4 J/cm^2 of total irradiation on the PI-coated substrates, no LC bulk alignment could be obtained from the substrates, but at 7.5 J/cm^2 or more, good LC bulk alignment was achieved. We then measured the SFG vibrational spectra for the PI surfaces irradiated by different UV dosages. Figure 3 shows how the peak strengths (A_q) of the phenylene C–C stretch in the SSP spectra decay with the UV dosage for LPL parallel and perpendicular to the incidence plane in SFG. In both cases, the data in Fig. 3 can be fit to an exponential decay, but the difference between the two, which denotes the photo-induced anisotropy, is rather small. The result suggests that such a substrate would yield a very weak azimuthal anchoring energy for an LC film deposited on it. This would also be manifested by a very weak anisotropy in an LC monolayer adsorbed on it. Indeed it has been reported that no anisotropy could be observed in second harmonic generation from an LC monolayer adsorbed on an LPL irradiated PI film.[19,28]

To study photo-induced anisotropy in bond breaking by LPL irradiation, it is more appropriate to use a PI surface that already has the main chains aligned. Such an alignment can be achieved by mechanical rubbing of the surface.[29] Figure 4 shows the SFG spectra of the phenylene skeleton stretch mode of PMDA–ODA before and after rubbing with the SSP polarization combination. The spectra taken with the incident plane parallel and antiparallel to the rubbing direction are significantly weaker than the one taken with the incident plane perpendicular to the rubbing direction. The result indicates that after rubbing, the phenylene rings of PMDA–ODA are preferentially oriented along the rubbing direction. It also suggests that the phenylene rings must, on average, incline at an angle with the surface plane. (If the rings lay flat in the surface plane, the phenylene modes would not be excited by the SSP polarization combination.) The spectra also show a weak forward-backward asymmetry along the rubbing direction. Again, fitting the spectra by Eqs. (1)–(6) yields the strength (A_q) for each mode in a given geometry. In the Appendix, we show how we can have a quantitative analysis of the spectral data and deduce an approximate orientational

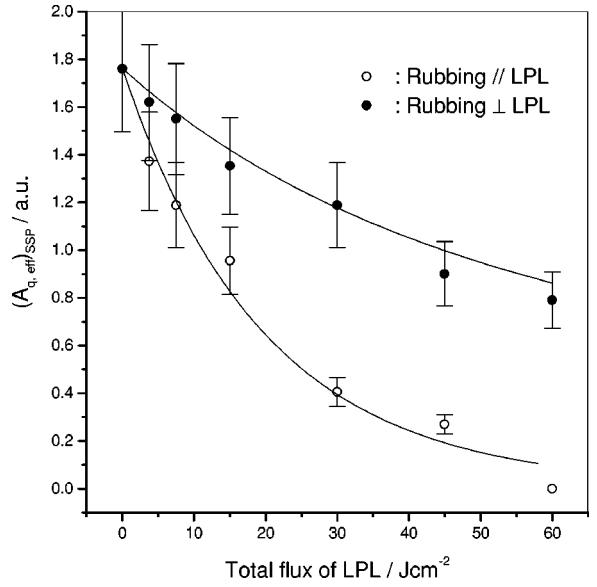

FIG. 5. Decays of the peak amplitude of the phenylene stretch mode for a rubbed PMDA–ODA film as functions of UV dosage with polarizations parallel (open circles) and perpendicular (filled circles) to the rubbing direction.

distribution function for the PI backbones lying on the rubbed surface.

Shown in Fig. 5 is how the peak strength of the phenylene skeleton stretch mode decreases with increase of UV irradiation. We present only the result obtained from the SSP spectra at $\Phi=90°$ (incidence plane perpendicular to the rubbing direction), taken on samples irradiated by LPL with polarization parallel and perpendicular to the rubbing direction, respectively. Decays of other spectra are similar, but most of them are too weak for the analysis to be accurate. As in Fig. 3, the experimental data in Fig. 5 can be described by exponential decays.

We can use a simple model to explain the result. We assume that the rate of bond breaking, κ, of a phenylene ring is directly proportional to the rate of UV excitation of PI. We then write[30,31]

$$\kappa=\alpha[(\hat{e}\cdot\hat{\xi}_1')^2+(\hat{e}\cdot\hat{\xi}_2')^2]+\beta[(\hat{e}\cdot\hat{\eta}_1')^2+(\hat{e}\cdot\hat{\eta}_2')^2], \quad (7)$$

where α and β are constant coefficients, $\hat{e}$ is the unit polarization vector of the UV irradiation, $(\xi_1',\eta_1',\zeta_1')$ and $(\xi_2',\eta_2',\zeta_2')$ are the molecular coordinates of the two phenylene rings shown in Fig. 6(a) with $(\xi_1'-\eta_1')$ and $(\xi_2'-\eta_2')$ describing the two ring planes, (ξ,η,ζ) in Fig. 6(a), refers to the coordinates of the molecular unit with $(\xi-\zeta)$ being the plane formed by the two axes of the two rings connected by the oxygen atom (ϕ–O–ϕ), and the angle δ_1 and δ_2 denote the inclinations of the two ring planes with respect to $(\xi-\eta)$ plane. For detailed analysis, we assume that the orientation of the two rings are correlated with $\delta_1=\delta_2=\delta$. In terms of the orientational angles of the rings and the molecular unit (Fig. 6), we have, for $\hat{e}=\hat{x}$ and $\hat{e}=\hat{y}$,

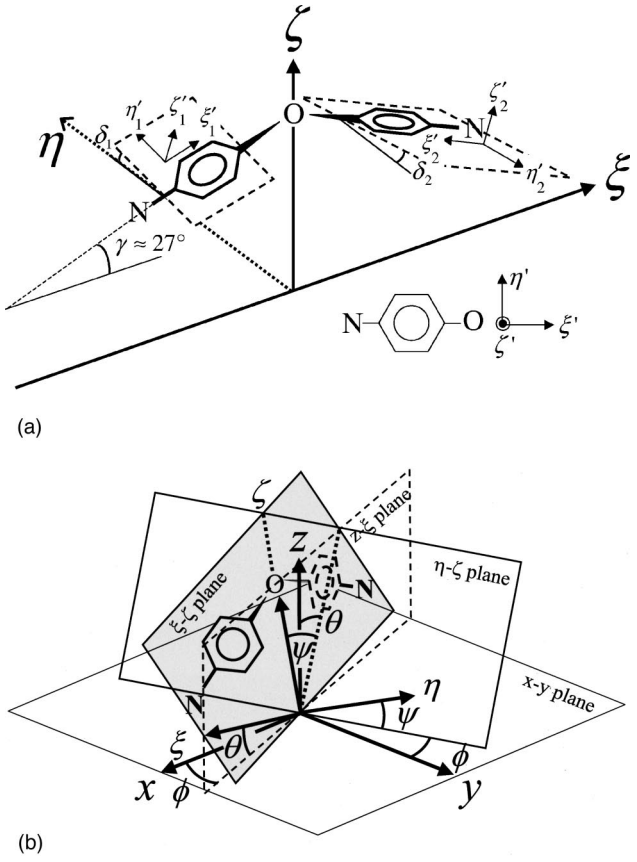

FIG. 6. (a) Geometry of a PMDA–ODA molecular unit. The coordinates of each phenylene ring are denoted by $(\xi_i',\eta_i',\zeta_i')$ with the ring lying in the plane of $(\xi_i'-\eta_i')$. The coordinates of the molecular unit are denoted by (ξ,η,ζ) with the long axes of the two rings forming a plane lying in $(\xi-\zeta)$. (b) Geometric relations between the molecular unit coordinates and the lab coordinates.

$$\kappa_x=2\alpha\cdot[(\cos\gamma\cos\theta-\sin\gamma\sin\theta\cos\psi)\cos\phi+\sin\gamma\sin\psi\sin\phi]^2+2\beta\cdot[\{-\sin\gamma\sin\delta\cos\theta-\sin\theta(\cos\gamma\sin\delta\cos\psi+\cos\delta\sin\psi)\}\cos\phi-(\cos\delta\cos\psi-\cos\gamma\sin\delta\sin\psi)\sin\phi]^2 \quad (\hat{e}=\hat{x}) \quad (8)$$

$$\kappa_y=2\alpha\cdot[(\cos\gamma\cos\theta-\sin\gamma\sin\theta\cos\psi)\sin\phi-\sin\gamma\sin\psi\cos\phi]^2+2\beta\cdot[\{-\sin\gamma\sin\delta\cos\theta-\sin\theta(\cos\gamma\sin\delta\cos\psi+\cos\delta\sin\psi)\}\sin\phi+(\cos\delta\cos\psi-\cos\gamma\sin\delta\sin\psi)\cos\phi]^2 \quad (\hat{e}=\hat{y}). \quad (9)$$

We now assume that the photo-induced bond breaking is equivalent to fragmentation of the molecular units. Let $f(\Omega,t)=N(\Omega,t)/N_0$ be the orientational distribution of the molecular units at time t with orientation specified by $\Omega(\theta,\phi,\psi,\delta)$ and $N_0=\int N(\Omega,t)d\Omega$ being the total surface density of molecular units. Then its decay with time is described by $df(\Omega,t)/dt=-\kappa(\hat{e},\Omega)f(\Omega,t)$, which has the solution

$$f(\Omega,t)=f(\Omega,0)\exp[-\kappa(\hat{e},\Omega)\cdot t]. \quad (10)$$

Knowing $f(\Omega,0)$ and some quantity $Q(t)=\int Q(\Omega)f(\Omega,t)d\Omega$ that exhibits the photo-induced effect, we can deduce the coefficients α and β.

In the Appendix, we describe how we can deduce an approximate $f(\Omega,0)$ from our SFG spectroscopic measurements of the rubbed PI surface. We obtain

$$f(\Omega,0)=C\exp\left[-\frac{(\theta-\theta_0)^2}{2\sigma_\theta^2}-\frac{(\phi-\phi_0)^2}{2\sigma_\phi^2}-\frac{(\psi-\psi_0)^2}{2\sigma_\psi^2}\right], \tag{11}$$

with $\theta_0=5°\pm2°$, $\phi_0=0°$, $\psi_0=0°$, $\sigma_\theta=6°\pm3°$, $\sigma_\phi=37°\pm3°$ and $\sigma_\psi=90°\pm89°$, and also $\delta=90°$. The quantity $Q(t)$ that suffers from photo-induced bond breaking in our case is the mode amplitude $A_{q,\mathrm{eff}}(\Phi=90°,\mathrm{SSP})$ for the phenylene stretch mode presented in Fig. 5. From Eq. (A2) in the Appendix, we find $A_{q,\mathrm{eff}}(\Phi=90°,\mathrm{SSP})\propto(A_q)_{xxz}$, and then using the expression of $(A_q)_{xxz}$ in Eq. (A3), we obtain

$$\begin{aligned}A_{q,\mathrm{eff}}(90°,\mathrm{SSP})=N_0(a_q)_{\zeta\zeta\zeta}\int&[\cos\theta\sin^2\phi\sin^2\psi\cos\psi\\&+\sin^2\theta\cos\theta\cos^2\phi\cos^3\psi]\\&\times f(\Omega,t)dt+N_0(a_q)_{\xi\xi\zeta}\\&\times\int[\cos^3\theta\cos^2\phi\cos\psi]f(\Omega,t)dt.\end{aligned} \tag{12}$$

Note that because $\delta=90°$, the $(a_q)_{\eta\eta\zeta}$ term in the expression of $(A_q)_{xxz}$ does not contribute. We can then use Eqs. (10) and (12) with α and β as adjustable parameters to fit the experimental data in Fig. 5, as shown by the solid curves in the figure. We find $\alpha=(3.0\pm0.3)\times10^{-2}$ $\mathrm{J^{-1}\cdot cm^2}$, $\beta=(2.6\pm0.2)\times10^{-2}$ $\mathrm{J^{-1}\cdot cm^2}$. The same coefficients and analysis applied to the unrubbed PI surface also describe the experimental data well, as shown in Fig. 3. The ratio $\alpha/\beta=1.15$ is in good agreement with that obtained by IR spectroscopy ($\alpha/\beta=1.23$).[19]

In conclusion, we have used SFG vibrational spectroscopy to probe UV photo-induced bond breaking and anisotropy on PMDA–ODA surfaces that allow good LC homogeneous alignment. We observe bond breaking of the PI backbones taking place in the part of the phenylene rings and imide core. The induced surface anisotropy is rather small, indicating that the azimuthal anchoring is weak. By analyzing the experimental results from a rubbed surface before and after the photo-induced bond breaking, we are able to deduce information about the surface orientations of the PI backbones and the photo–dissociation rates for UV irradiation polarized parallel and perpendicular to the PI backbones.

ACKNOWLEDGMENTS

This work was supported by U.S. National Science Foundation (NSF) Grant No. DMR-0075402 and partially by Hitachi, Ltd. One of the authors (M.O.) acknowledges the financial support by Hitachi, Ltd. The authors greatly appreciate the support by Junji Tanno of Hitachi, Ltd. Displays, for sample preparation. Thanks are also due to Dr. Takao Miwa of Hitachi Research Laboratory for providing us with PMDA–ODA.

TABLE I. Parameters used in the calculation of $(A_q)_{ijk}$.

	ω_{SF}	ω_{vis}	ω_{IR}
Wavelength λ/μm	0.492	0.532	6.60
Refractive index n	1.463	1.461	1.186
Beam angle β/deg	45.8	45.0	57.0
Fresnel factor L_{xx}	0.922	0.917	1.045
Fresnel factor L_{yy}	0.707	0.712	0.787
Fresnel factor L_{zz}	$1.078/\epsilon'_{\mathrm{SF}}$	$1.083/\epsilon'_{\mathrm{vis}}$	$0.955/\epsilon'_{\mathrm{IR}}$

APPENDIX

In the quantitative analysis to find $f(\Omega,0)$ on a rubbed surface, we need to obtain values of $(A_q)_{ijk}$ that can be deduced from the SFG spectral data. For a rubbed surface with the rubbing direction along x (and the surface normal along z), the C_2 symmetry allows 10 independent nonvanishing elements of $(A_q)_{ijk}$. They are[32]

$$\begin{aligned}&(A_q)_{xxz},\ (A_q)_{yyz},\ (A_q)_{zzz},\ (A_q)_{xzx}=(A_q)_{zxx},\\&(A_q)_{yzy}=(A_q)_{zyy},\ (A_q)_{xxx},\ (A_q)_{yyx},\ (A_q)_{zzx},\\&(A_q)_{xyy}=(A_q)_{yxy},\ (A_q)_{xzz}=(A_q)_{zxz}.\end{aligned} \tag{A1}$$

The last five elements would vanish if the forward–backward symmetry along x also holds. We can determine the values of these nonvanishing $(A_q)_{ijk}$ from the experimentally deduced values of $A_{q,\mathrm{eff}}$ for different azimuthal sample orientations Φ and input/output polarization combinations using Eq. (2) which remains valid if $\chi^{(2)}$ is replaced by A_q. For example, with the forward–backward asymmetry neglected, Eq. (2) yields

$$\begin{aligned}&A_{q,\mathrm{eff}}(\Phi,\mathrm{SSP})\\&\quad=L_{yy}(\omega_{\mathrm{SF}})L_{yy}(\omega_{\mathrm{vis}})L_{zz}(\omega_{\mathrm{ir}})\sin\beta_{\mathrm{ir}}\\&\qquad\times[(A_q)_{yyz}\cos^2\Phi+(A_q)_{xxz}\sin^2\Phi],\\&A_{q,\mathrm{eff}}(\Phi,\mathrm{SPS})\\&\quad=L_{yy}(\omega_{\mathrm{SF}})L_{zz}(\omega_{\mathrm{vis}})L_{yy}(\omega_{\mathrm{ir}})\sin\beta_{\mathrm{vis}}\\&\qquad\times[(A_q)_{yzy}\cos^2\Phi+(A_q)_{xzx}\sin^2\Phi],\\&A_{q,\mathrm{eff}}(\Phi,\mathrm{PPP})\\&\quad=-L_{xx}(\omega_{\mathrm{SF}})L_{xx}(\omega_{\mathrm{vis}})L_{zz}(\omega_{\mathrm{ir}})\cos\beta_{\mathrm{SF}}\cos\beta_{\mathrm{vis}}\sin\beta_{\mathrm{ir}}\\&\qquad\times[(A_q)_{xxz}\cos^2\Phi+(A_q)_{yyz}\sin^2\Phi]+L_{zz}(\omega_{\mathrm{SF}})\\&\qquad\times L_{zz}(\omega_{\mathrm{vis}})L_{zz}(\omega_{\mathrm{ir}})\sin\beta_{\mathrm{SF}}\sin\beta_{\mathrm{vis}}\sin\beta_{\mathrm{ir}}(A_q)_{zzz}.\end{aligned} \tag{A2}$$

The values of $A_{q,\mathrm{eff}}(\Phi)$ for different Φ and different polarization combinations can be deduced by fitting the measured SFG spectra using Eqs. (1)–(6) and knowing that the spectral peak positions and profiles were independent of Φ. In the calculation, the Fresnel factors L used were those for the air/fused quartz interface (listed in Table I). The effect of the PI film on the Fresnel factors was negligible because the film was very thin (25 nm). For the interfacial dielectric con-

TABLE II. Measured and calculated nonvanishing tensor elements $(A_q)_{ijk}$ for the phenylene skeleton C–C stretch mode.

	Measured	Calculated
A_{xxz}	5.2±0.2	5.4
A_{yyz}	2.2±0.2	2.3
A_{zzz}	1.6±0.3	1.4
$A_{xzx}=A_{zxx}$	−0.7±0.3	−0.4
$A_{yzy}=A_{zyy}$	~0	−0.2
A_{xxx}	0.8±0.1	0.8
A_{yyx}	0.1±0.1	0.2
A_{zzx}	0.2±0.1	0.2
$A_{xyy}=A_{yxy}$	~0	0.2
$A_{xzz}=A_{zxz}$	~0	−0.8

TABLE III. Parameters used to calculated $\chi^{(2)}_{\text{eff}}$ of a z-cut quartz crystal. For convenience the birefringence of the crystal is neglected, and the refractive index of the ordinary wave n_o is used for all polarizations. For the bulk nonlinearity of quartz, we neglect the dispersion and take $\chi^{(2)}_{\text{q}} \approx 1.6\times10^{-12}$ m/V.[34] The coherence length is $l_c \approx 27$ nm.

	ω_{SF}	ω_{vis}	ω_{IR}
Wavelength λ/μm	0.492	0.532	6.60
Refractive index $n=n_o$	1.549	1.547	1.226
Beam angle β/deg	45.8	45.0	57.0
Fresnel factor L_{xx}	0.902	0.897	1.044
Fresnel factor L_{yy}	0.673	0.679	0.757

stant ϵ', we adopted the approach of Ref. 32 and found the optimum values for ϵ'. They are $\epsilon'_{\text{SF}} \approx \epsilon'_{\text{vis}} \approx 2.1$ and $\epsilon'_{\text{IR}} \approx 1.2$.

Following the above procedure, we first obtained for the rubbed PMDA–ODA surface the values of the first five elements in Eq. (A1) by neglecting the weak forward-backward asymmetry, and then the values of the other five elements with the forward-backward asymmetry taken as a perturbation. The results are given in Table II.

To find an approximate $f(\Omega,0)$, we need the explicit expressions for $A_{q,ijk}$ or $(a_q)_{ijk}(\Omega)$ in terms of Ω [see the relations between A_q and $a_q(\Omega)$ in Eq. (6)]. As described in Fig. 6(a), each molecular unit of PMDA–ODA consists of two phenylene rings, which are symmetrically oriented with respect to ζ axis. For each ring, only two elements of $(a_q)_{lmn}$ are nonvanishing, $(a_q)_{\xi'\xi'\xi'}$ and $(a_q)_{\eta'\eta'\xi'}$ because only the IR component along $\hat{\xi}'$ can excite the skeleton stretch mode of the ring. (Displayed in the inset of Fig. 2 is the ν_{19a} mode of 1, 4-disubstituted benzene that resembles the phenylene skeleton stretch mode.[33]) For the molecular unit, symmetry requires that the dominant components of a_q be $(a_q)_{\zeta\zeta\zeta}$, $(a_q)_{\xi\xi\xi}$ and $(a_q)_{\eta\eta\zeta}$. Assuming $\delta_1=\delta_2=\delta$, we have, in the coordinates of the molecular unit,

$$
\begin{aligned}
(a_q)_{\zeta\zeta\zeta} &= 2(a_q)_{\xi'\xi'\xi'}\sin^3\gamma \\
&\quad + 2(a_q)_{\eta'\eta'\xi'}\sin\gamma\cos^2\gamma\sin^2\delta, \\
(a_q)_{\xi\xi\zeta} &= 2(a_q)_{\xi'\xi'\xi'}\sin\gamma\cos^2\gamma \\
&\quad + 2(a_q)_{\eta'\eta'\xi'}\sin^3\gamma\sin^2\delta, \\
(a_q)_{\eta\eta\zeta} &= 2(a_q)_{\eta'\eta'\xi'}\sin\gamma\cos^2\delta.
\end{aligned}
\tag{A3}
$$

Now let the orientation of each molecular unit in the lab coordinates be represented by $\Omega=(\theta,\phi,\psi)$, defined in Fig. 6(b). We find, from Eq. (6),

$$
\begin{aligned}
(A_q)_{xxz} &= (a_q)_{\zeta\zeta\zeta}\langle\cos\theta\sin^2\phi\sin^2\psi\cos\psi \\
&\quad + \sin^2\theta\cos\theta\cos^2\phi\cos^3\psi\rangle \\
&\quad + (a_q)_{\xi\xi\zeta}\langle\cos^3\theta\cos^2\phi\cos\psi\rangle \\
&\quad + (a_q)_{\eta\eta\zeta}\langle\cos\theta\sin^2\phi\cos^3\psi \\
&\quad + \sin^2\theta\cos\theta\cos^2\phi\sin^2\psi\cos\psi\rangle, \\
(A_q)_{yyz} &= (a_q)_{\zeta\zeta\zeta}\langle\cos\theta\cos^2\phi\sin^2\psi\cos\psi \\
&\quad + \sin^2\theta\cos\theta\sin^2\phi\cos^3\psi\rangle \\
&\quad + (a_q)_{\xi\xi\zeta}\langle\cos^3\theta\sin^2\phi\cos\psi\rangle \\
&\quad + (a_q)_{\eta\eta\zeta}\langle\cos\theta\cos^2\phi\cos^3\psi \\
&\quad + \sin^2\theta\cos\theta\sin^2\phi\sin^2\psi\cos\psi\rangle, \\
(A_q)_{zzz} &= (a_q)_{\zeta\zeta\zeta}\langle\cos^3\theta\cos^3\psi\rangle \\
&\quad + (a_q)_{\xi\xi\zeta}\langle\sin^2\theta\cos\theta\cos\psi\rangle \\
&\quad + (a_q)_{\eta\eta\zeta}\langle\cos^3\theta\sin^2\psi\cos\psi\rangle, \\
(A_q)_{xzx} &= (a_q)_{\zeta\zeta\zeta}\langle\cos\theta\sin^2\phi\sin^2\psi\cos\psi \\
&\quad + \sin^2\theta\cos\theta\cos^2\phi\cos^3\psi\rangle \\
&\quad - (a_q)_{\xi\xi\zeta}\langle\sin^2\theta\cos\theta\cos^2\phi\cos\psi\rangle \\
&\quad - (a_q)_{\eta\eta\zeta}\langle\cos\theta\sin^2\phi\sin^2\psi\cos\psi \\
&\quad - \sin^2\theta\cos\theta\cos^2\phi\sin^2\psi\cos\psi\rangle, \\
(A_q)_{yzy} &= (a_q)_{\zeta\zeta\zeta}\langle\cos\theta\cos^2\phi\sin^2\psi\cos\psi \\
&\quad + \sin^2\theta\cos\theta\sin^2\phi\cos^3\psi\rangle \\
&\quad - (a_q)_{\xi\xi\zeta}\langle\sin^2\theta\cos\theta\sin^2\phi\cos\psi\rangle \\
&\quad - (a_q)_{\eta\eta\zeta}\langle\cos\theta\cos^2\phi\sin^2\psi\cos\psi \\
&\quad - \sin^2\theta\cos\theta\sin^2\phi\sin^2\psi\cos\psi\rangle,
\end{aligned}
\tag{A4}
$$

and five other similar equations for the five other $(A_q)_{ijk}$ elements that would vanish with forward–backward symmetry. Here, $\langle Q(\Omega)\rangle \equiv \int Q(\Omega) f(\Omega,0)\, d\Omega$. For the phenylene skeleton stretch mode, it can be shown from Eq. (A4) that

$$
\begin{aligned}
&(A_q)_{xxz} + (A_q)_{yyz} - (A_q)_{xzx} - (A_q)_{yzy} \\
&\quad = [(a_q)_{\xi\xi\zeta} + (a_q)_{\eta\eta\zeta}]\langle\cos\theta\cos\psi\rangle, \\
&(A_q)_{xzx} + (A_q)_{yzy} + (A_q)_{zzz} = (a_q)_{\zeta\zeta\zeta}\langle\cos\theta\cos\psi\rangle.
\end{aligned}
\tag{A5}
$$

Knowing $(A_q)_{ijk}$, we can then use the last equation in Eq. (6) to find an approximate expression for $f(\Omega,0)$. We assume $f(\Omega,0)$ takes a Gaussian form

$$
f(\Omega,0) = C\exp\left[-\frac{(\theta-\theta_0)^2}{2\sigma_\theta^2} - \frac{(\phi-\phi_0)^2}{2\sigma_\phi^2} - \frac{(\psi-\psi_0)^2}{2\sigma_\psi^2}\right],
\tag{A6}
$$

where C is a normalization constant and θ_0, ϕ_0, ψ_0, σ_θ, σ_ϕ, and σ_ψ are parameters to be determined. In our calculations for the rubbed PI, we first neglect the small forward-backward asymmetry and therefore we have $\theta_0=0°$. Knowing the values of the five $A_{q,ijk}$ in Eq. (A4), listed in Table II, we can then use Eqs. (A3) and (A4) to determine the parameters σ_θ, σ_ϕ, σ_ψ, δ and $(a_q)_{\eta'\eta'\xi'}/(a_q)_{\xi'\xi'\xi'}$. We find $\delta=90°$, $(a_q)_{\eta'\eta'\xi'}/(a_q)_{\xi'\xi'\xi'}=-6.5\pm0.3$, $\sigma_\theta=6°\pm3°$, $\sigma_\phi=37°\pm3°$, and $\psi_0=0°\pm90°$ with σ_ψ varying from $\sim90°$ at $\psi_0=0°$ to $\sim180°$ at $\psi_0=\pm90°$. The values of ψ_0 and σ_ψ suggest that the phenylene ring plane is inclined towards the surface plane with a rather broad distribution. If the forward-backward asymmetry of the experimental data listed in Table II is included in the analysis, we obtain $\theta_0=5°\pm2°$ with the other parameters hardly changed. To show consistency of the results, we have used the deduced $f(\Omega,0)$ to re-evaluate $(A_q)_{ijk}$. The calculated values of $(A_q)_{ijk}$, also listed in Table II, are indeed close to those deduced from our measurement.

[1] C. Mauguin, Bull. Soc. Fr. Mineral. **34**, 71 (1911).
[2] J. Cognard, Mol. Cryst. Liq. Cryst. **51**, 1 (1982).
[3] J. M. Geary, J. W. Goodby, A. R. Kmetz, and J. S. Patel, J. Appl. Phys. **62**, 4100 (1987).
[4] N. A. J. M. van Aerle, M. Barmentlo, and R. W. J. Hollering, J. Appl. Phys. **74**, 3111 (1993).
[5] X. Zhuang, L. Marrucci, and Y. R. Shen, Phys. Rev. Lett. **73**, 1513 (1994).
[6] K. Sawa, K. Sumiyoshi, Y. Hirai, K. Tateishi, and T. Kamejima, Jpn. J. Appl. Phys., Part 1 **33**, 6273 (1994).
[7] Y. Ouchi, I. Mori, M. Sei, E. Ito, T. Araki, H. Ishii, K. Seki, and K. Kondo, Physica B **208/209**, 407 (1995).
[8] M. F. Toney, T. P. Russell, J. A. Logan, H. Kikuchi, J. M. Sands, and S. K. Kumar, Nature (London) **374**, 709 (1995).
[9] I. Hirosawa, Jpn. J. Appl. Phys., Part 1 **35**, 5873 (1996).
[10] K. Ichimura, Y. Suzuki, T. Seki, A. Hosoki, and K. Aoki, Langmuir **4**, 1214 (1988).
[11] G. W. Gibbons, P. Shannon, S. Sun, and B. Swetlin, Nature (London) **351**, 49 (1991).
[12] M. Schadt, K. Schmitt, V. Hozinkov, and V. Chifrinnov, Jpn. J. Appl. Phys., Part 1 **31**, 2155 (1992).
[13] Y. Iimura, T. Saitoh, S. Kobayashi, and T. Hashimoto, J. Photopolym. Sci. Technol. **8**, 257 (1995).
[14] M. Schadt, H. Seiberle, and A. Schuster, Nature (London) **381**, 212 (1996).
[15] M. Hasegawa and Y. Taira, J. Photopolym. Sci. Technol. **8**, 241 (1995).
[16] D. C. Rich, E. Sichel, and P. Cebe, J. Appl. Polym. Sci. **65**, 1151 (1997).
[17] Y. Wang, A. Kanazawa, T. Shiono, T. Ikeda, Y. Matsuki, and Y. Takeuchi, Appl. Phys. Lett. **72**, 545 (1998).
[18] M. Hasegawa, Jpn. J. Appl. Phys., Part 2 **38**, L457 (1999).
[19] K. Sakamoto, K. Usami, M. Watanabe, R. Arafune, and S. Ushioda, Appl. Phys. Lett. **72**, 1832 (1998).
[20] Y. Wang, C. Xu, A. Kanazawa, T. Shiono, T. Ikeda, Y. Matuski, and Y. Takeuchi, J. Appl. Phys. **84**, 4573 (1998).
[21] Y. R. Shen, in *Proceedings of the International School of Physics "Enrico Fermi," Course CXX, Frontier in Laser Spectroscopy*, edited by T. W. Hansch and M. Inguscio (North-Holland, Amsterdam, 1994), p. 139.
[22] Y. R. Shen, Surf. Sci. **299/300**, 551 (1994).
[23] Y. R. Shen, *The Principle of Nonlinear Optics* (Wiley, New York, 1984).
[24] Y. R. Shen, Annu. Rev. Phys. Chem. **40**, 327 (1989).
[25] Y. R. Shen, in *Nonlinear Spectroscopy for Molecular Structure Determination*, edited by R. W. Field, E. Hirota, J. P. Maier, and S. Tsuchiya, IUPAC Chemical Data Series (Blackwell Science, Oxford, UK, 1998), Ch. 10.
[26] H. Ishida, S. T. Wellinghoff, E. Baer, and J. L. Koenig, Macromolecules **13**, 826 (1980).
[27] S. Gong, J. Kanicki, L. Ma, and J. Z. Z. Zhong, Jpn. J. Appl. Phys., Part 1 **38**, 5996 (1999).
[28] K. Kumagai, K. Sakamoto, K. Usami, R. Arafune, Y. Nakabayashi, and S. Ushioda, Jpn. J. Appl. Phys., Part 1 **38**, 3615 (1999).
[29] M. Oh-e, S.-C. Hong, and Y. R. Shen, J. Phys. Chem. B **104**, 7455 (2000).
[30] J. Chen, D. L. Johnson, P. J. Bos, X. Wang, and J. L. West, Phys. Rev. E **54**, 1599 (1996).
[31] A. Th. Ionescu, R. Barberi, M. Giocondo, M. Iovane, and A. L. Alexe-Ionescu, Phys. Rev. E **58**, 1967 (1998).
[32] X. Wei, S.-C. Hong, X. Zhuang, T. Goto, and Y. R. Shen, Phys. Rev. E **62**, 5160 (2000).
[33] G. Varsányi, *Assignments for Vibrational Spectra of Seven Hundred Benzene Derivatives* (Wiley, New York, 1974), Vol. 1.
[34] S. Singh, in *Handbook of Lasers*, edited by R. J. Pressley (RC, Cleveland, OH, 1971), p. 489 and p. 497.